JOC The Journal of Organic Chemistry

Article

Reaction of Phenols with the 2,2-Diphenyl-1-picrylhydrazyl Radical. Kinetics and DFT Calculations Applied To Determine ArO-H Bond Dissociation Enthalpies and Reaction Mechanism

Mario C. Foti, Carmelo Daquino, Iain D. Mackie, Gino A. DiLabio, and K. U. Ingold

J. Org. Chem., **2008**, 73 (23), 9270-9282 • DOI: 10.1021/jo8016555 • Publication Date (Web): 08 November 2008

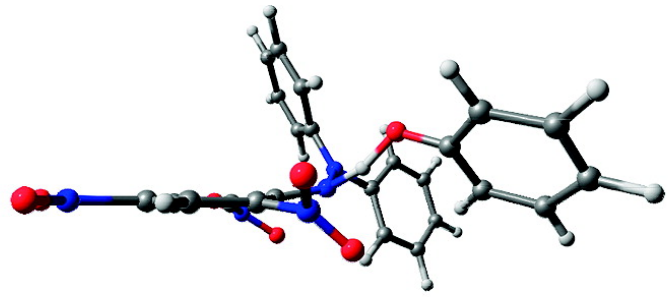

Transition state structure of Phenol + **dpph•**

More About This Article

Additional resources and features associated with this article are available within the HTML version:

- Supporting Information
- Access to high resolution figures
- Links to articles and content related to this article
- Copyright permission to reproduce figures and/or text from this article

View the Full Text HTML

JOC Article

Reaction of Phenols with the 2,2-Diphenyl-1-picrylhydrazyl Radical. Kinetics and DFT Calculations Applied To Determine ArO-H Bond Dissociation Enthalpies and Reaction Mechanism

Mario C. Foti,*,† Carmelo Daquino,† Iain D. Mackie,‡ Gino A. DiLabio,*,‡ and K. U. Ingold§

Istituto di Chimica Biomolecolare del CNR, Via del Santuario 110, I-95028 Valverde (CT) Italy, National Institute for Nanotechnology, National Research Council of Canada 11421 Saskatchewan Drive, Edmonton, AB, Canada T6G 2M9, and National Research Council of Canada, 100 Sussex Drive, Ottawa, ON, Canada K1A 0R6

mario.foti@icb.cnr.it; gino.dilabio@nrc-cnrc.gc.ca

Received August 12, 2008

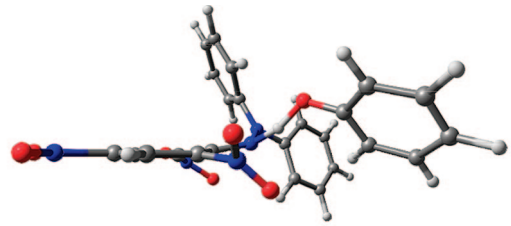

Transition state structure of Phenol + **dpph•**

The formal H-atom abstraction by the 2,2-diphenyl-1-picrylhydrazyl (**dpph•**) radical from 27 phenols and two unsaturated hydrocarbons has been investigated by a combination of kinetic measurements in apolar solvents and density functional theory (DFT). The computed minimum energy structure of **dpph•** shows that the access to its divalent N is strongly hindered by an ortho H atom on each of the phenyl rings and by the *o*-NO_2 groups of the picryl ring. Remarkably small Arrhenius pre-exponential factors for the phenols [range $(1.3-19) \times 10^5$ M^{-1} s^{-1}] are attributed to steric effects. Indeed, the entropy barrier accounts for up to ca. 70% of the free-energy barrier to reaction. Nevertheless, rate differences for different phenols are largely due to differences in the activation energy, $E_{a,1}$ (range 2 to 10 kcal/mol). In phenols, electronic effects of the substituents and intramolecular H-bonds have a large influence on the activation energies and on the ArO-H BDEs. There is a *linear* Evans−Polanyi relationship between $E_{a,1}$ and the ArO-H BDEs: $E_{a,1}$/kcal × $mol^{-1} = 0.918$ BDE(ArO-H)/kcal × $mol^{-1} - 70.273$. The proportionality constant, 0.918, is large and implies a "late" or "product-like" transition state (TS), a conclusion that is congruent with the small deuterium kinetic isotope effects (range 1.3−3.3). This Evans−Polanyi relationship, though questionable on theoretical grounds, has profitably been used to estimate several ArO-H BDEs. Experimental ArO-H BDEs are generally in good agreement with the DFT calculations. Significant deviations between experimental and DFT calculated ArO-H BDEs were found, however, when an intramolecular H-bond to the O• center was present in the phenoxyl radical, e.g., in ortho semiquinone radicals. In these cases, the coupled cluster with single and double excitations correlated wave function technique with complete basis set extrapolation gave excellent results. The TSs for the reactions of **dpph•** with phenol, 3- and 4-methoxyphenol, and 1,4-cyclohexadiene were also computed. Surprisingly, these TS structures for the phenols show that the reactions cannot be described as occurring exclusively by either a HAT or a PCET mechanism, while with 1,4-cyclohexadiene the PCET character in the reaction coordinate is much better defined and shows a strong $\pi-\pi$ stacking interaction between the incipient cyclohexadienyl radical and a phenyl ring of the **dpph•** radical.

Introduction

The nitrogen-centered radical 2,2-diphenyl-1-picrylhydrazyl (**dpph•**)[1] has been extensively employed in kinetic studies of hydrogen-atom abstractions from carbon,[2] nitrogen,[3] sulfur,[4] and oxygen,[5,6] particularly from phenols.[5] This radical is popular[7]

† Istituto di Chimica Biomolecolare del CNR.

‡ National Institute for Nanotechnology.

§ National Research Council of Canada.

10.1021/jo8016555 CCC: $40.75
Published on Web 11/08/2008

for such studies because it is monomeric in solution and air stable,[1] is commercially available, and is strongly colored. This last property allows the course of reaction to be monitored using conventional UV−vis spectroscopy. Phenols (ArOH) have been favored substrates for study, frequently because their reactions with **dpph**$^{\bullet}$ (reaction 1) are presumed to be similar to those important in their antioxidant reactions with peroxyl radicals, ROO$^{\bullet}$ (reaction 2). However, the thermodynamics of H-atom abstraction and the steric requirements of these two radicals are very different. Indeed, peroxyl radicals usually react with any particular phenol some 3 orders of magnitude more rapidly than does **dpph**$^{\bullet}$.[5a] The divalent nitrogen of **dpph**$^{\bullet}$ is sterically shielded (vide infra), which reduces this radical's reactivity and, in H-atom abstractions from phenols, produces unusually small Arrhenius factors,[5a] range $4.5 \times 10^3 - 1.9 \times 10^6$ M^{-1} s^{-1}, whereas "normal" values of A for H-atom abstractions are generally considered to be about $10^{8.5}$ M^{-1} s^{-1}.[8] The N−H bond dissociation enthalpy (BDE) of **dpph**-H is ∼78.9 kcal/mol,[5a] and for most phenols, reaction 1 will be endothermic and slower than its reverse (reaction −1), whereas reaction 2 will be exothermic for many phenols[9] and faster than its reverse (reaction −2). The entropy changes in reactions 1 and 2 are negligible; therefore, $\Delta G_1 \approx \Delta H_1$ and $\Delta G_2 \approx \Delta H_2$.[5a,10]

$$\mathrm{ArOH} + \mathbf{dpph}^{\bullet} \rightleftarrows \mathrm{ArO}^{\bullet} + \mathbf{dpph}\text{-H} \quad (1)$$

$$\mathrm{ArOH} + \mathrm{ROO}^{\bullet} \rightleftarrows \mathrm{ArO}^{\bullet} + \mathrm{ROOH} \quad (2)$$

Formal H-atom abstractions from phenols, ArOH + Y$^{\bullet}$ ⇄ ArO$^{\bullet}$ + YH, are now recognized to proceed by four different mechanisms:[11] hydrogen-atom transfer (HAT), proton-coupled electron-transfer (PCET),[12] sequential proton-loss electron-transfer (SPLET),[5c−e] and electron-transfer proton-loss (ET-PT) with the proton being initially transferred to a solvent molecule to which the phenol is hydrogen-bonded.[13] In the HAT mechanism, the proton together with one of its two bonding electrons are transferred to Y$^{\bullet}$. In the PCET mechanism of phenol oxidation by a Y$^{\bullet}$ radical that possesses one, or more, lone pairs of electrons on the atom that (formally) bears the unpaired electron (i.e., the radical center), a pretransition state (pre-TS), hydrogen-bonded complex is formed between the OH and a lone pair on Y$^{\bullet}$. The proton is then transferred from its two bonding electrons to the radical's lone pair with the accompanying electron moving from the 2p lone pair on the phenol's oxygen atom to the radical's singly occupied molecular orbital (SOMO). The formation of a complex with a hydrogen bond (HB) between ArOH and Y$^{\bullet}$ causes the reaction to be entropically disfavored ($\Delta S_{HB} \approx -11$ cal/mol·K).[14] However, formation of a HB complex also has effects that strongly favor reaction, whether by the HAT or PCET mechanism. Thus, the formation of the pre-TS HB complex causes the O atom in ArOH and the Y$^{\bullet}$ radical center to approach each other more closely than they would if a HB was not formed. Since the intersecting ArO-H and Y-H Morse-like potential energy curves have their minima closer together, the difference in enthalpy between the pre-TS HB complex and the TS is smaller than the corresponding enthalpy difference for the same reaction occurring without HB formation. Furthermore, with a pre-TS HB complex, the barrier to reaction will not only be lower, it will also be narrower than in the absence of HB formation. The narrower barrier will enhance the reaction rate by enhancing quantum-mechanical tunnelling of the proton and electron. Finally, proton transfer in the HB complex will be a first-order process and, as such, will generally have an enhanced pre-exponential factor compared with a second-order reaction.[15]

One question we address in the present work, using a combination of experimental kinetic work and theoretical calculations, is: *Does H-atom abstraction by* **dpph**$^{\bullet}$ *from phenols, reaction 1*, occur by the HAT or PCET mechanism? From the experimental side, this question relates only to reactions carried out in alkane solvents where neither the SPLET nor the ETPT mechanism can occur. Both the HAT and PCET mechanisms will be disfavored by steric congestion around the divalent nitrogen atom. HAT and PCET are also likely to be disfavored by the fact that there are other hydrogen bond accepting groups in **dpph**$^{\bullet}$ (e.g., the three nitro groups) to which the phenol might preferentially hydrogen bond, particularly since the electron withdrawing picryl group will make the divalent nitrogen electron-deficient. The results of DFT calculations on the transition state for reaction 1 provide fundamental insights into the HAT vs PCET reaction mechanism.

Our earlier experimental work[5a] has been significantly expanded. Arrhenius parameters for hydrogen atom abstraction from 27 phenols (see Chart 1) in saturated hydrocarbon solvents are now reported. These activation enthalpies were used to estimate ArO-H bond dissociation enthalpies (BDEs) for many of the phenols and these ArO-H BDEs are shown to be in good agreement with literature values and with the results of DFT calculations.

Results

Experimental Study of the Kinetics of Reaction 1. The **dpph**$^{\bullet}$ radical absorbs strongly in the visible part of the spectrum and in apolar solvents, $\lambda_{max} \approx 512$ nm and $\epsilon_{max} \approx 12000$ M^{-1}

(1) Goldschmidt, S.; Renn, K. *Ber. Chem.* **1922**, *55B*, 628–643. Walter, R. I. *J. Am. Chem. Soc.* **1966**, *88*, 1930–1937.
(2) Valgimigli, L.; Ingold, K. U.; Lusztyk, J. *J. Org. Chem.* **1996**, *61*, 7947–7950. Pitts, J. N.; Schuck, E. A.; Wan, J. K. S. *J. Am. Chem. Soc.* **1964**, *86*, 296–297. Kubo, J. *Ind. Eng. Chem. Res.* **1998**, *37*, 4492–4500. (d) Baciocchi, E.; Calcagni, A.; Lanzalunga, O. *J. Org. Chem.* **2008**, *73*, 4110–4115.
(3) Mulder, P.; Litwinienko, G.; Shuqiong, L.; MacLean, P. D.; Barclay, L. R. C.; Ingold, K. U. *Chem. Res. Toxicol.* **2006**, *19*, 79–85. McGowan, J. C.; Powell, T.; Raw, R. *J. Chem. Soc.* **1959**, 3103–3110.
(4) Russell, K. E. *J. Phys. Chem.* **1954**, *58*, 437–439. Ewald, A. H. *Trans. Faraday Soc.* **1959**, *55*, 792–797.
(5) (a) Foti, M. C.; Daquino, C. *Chem. Commun.* **2006**, 3252–3254. (b) Foti, M. C.; Daquino, C.; Geraci, C. *J. Org. Chem.* **2004**, *69*, 2309–2314. (c) Litwinienko, G.; Ingold, K. U. *J. Org. Chem.* **2003**, *68*, 3433–3438. (d) Litwinienko, G.; Ingold, K. U. *J. Org. Chem.* **2004**, *69*, 5888–5896. (e) Litwinienko, G.; Ingold, K. U. *J. Org. Chem.* **2005**, *70*, 8982–8990.
(6) Astolfi, P.; Greci, L.; Paul, T.; Ingold, K. U. *J. Chem. Soc., Perkin Trans. 2* **2001**, 1631–1633.
(7) SciFinder currently gives 6811 references with the keyword "**dpph**".
(8) Benson, S. W. *Thermochemical Kinetics*, 2nd ed.; Wiley: New York, 1976.
(9) The BDE of ROO-H is relatively constant, 86−88 kcal/mol.
(10) (a) Lucarini, M.; Pedulli, G. F.; Cipollone, M. *J. Org. Chem.* **1994**, *59*, 5063–5070. (b) Lucarini, M.; Pedrielli, P.; Peduli, G. F.; Cabiddu, S.; Fattuoni, C. *J. Org. Chem.* **1996**, *61*, 9259–9263.
(11) Litwinienko, G.; Ingold, K. U. *Acc. Chem. Res.* **2007**, *40*, 222–230.
(12) (a) Mayer, J. M.; Hrovat, D. A.; Thomas, J. L.; Borden, W. T. *J. Am. Chem. Soc.* **2002**, *124*, 11142–11147. (b) DiLabio, G. A.; Johnson, E. R *J. Am. Chem. Soc.* **2007**, *129*, 6199–6203v. (c) Tishchenko, O.; Truhlar, D. G.; Ceulemans, A.; Nguyen, M. T. *J. Am. Chem. Soc.* **2008**, *130*, 7000–7010.
(13) Galian, R. E.; Litwinienko, G.; Perez-Prieto, J.; Ingold, K. U. *J. Am. Chem. Soc.* **2007**, *129*, 9280–9281.
(14) de Heer, M. I.; Korth, H-G.; Mulder, P. *J. Org. Chem.* **1999**, *64*, 6969–6975.
(15) Although the rate constant expression derived from Transition State Theory does not contain any explicit term related to a pre-TS complex, the pre-TS complex does influence the activation energy through a tunnelling factor. See: Uc, V. H.; Alvarez-Idaboy, J. R.; Galano, A.; Garcia-Cruz, I.; Vivier-Bunge, A. *J. Phys. Chem. A* **2006**, *110*, 10155–10162, and cited references. Donahue, N. M *Chem. Rev.* **2003**, *103*, 4593–4604.

CHART 1. Structures of 27 Phenols and Two Hydrocarbons Employed in the Current Kinetic Studies

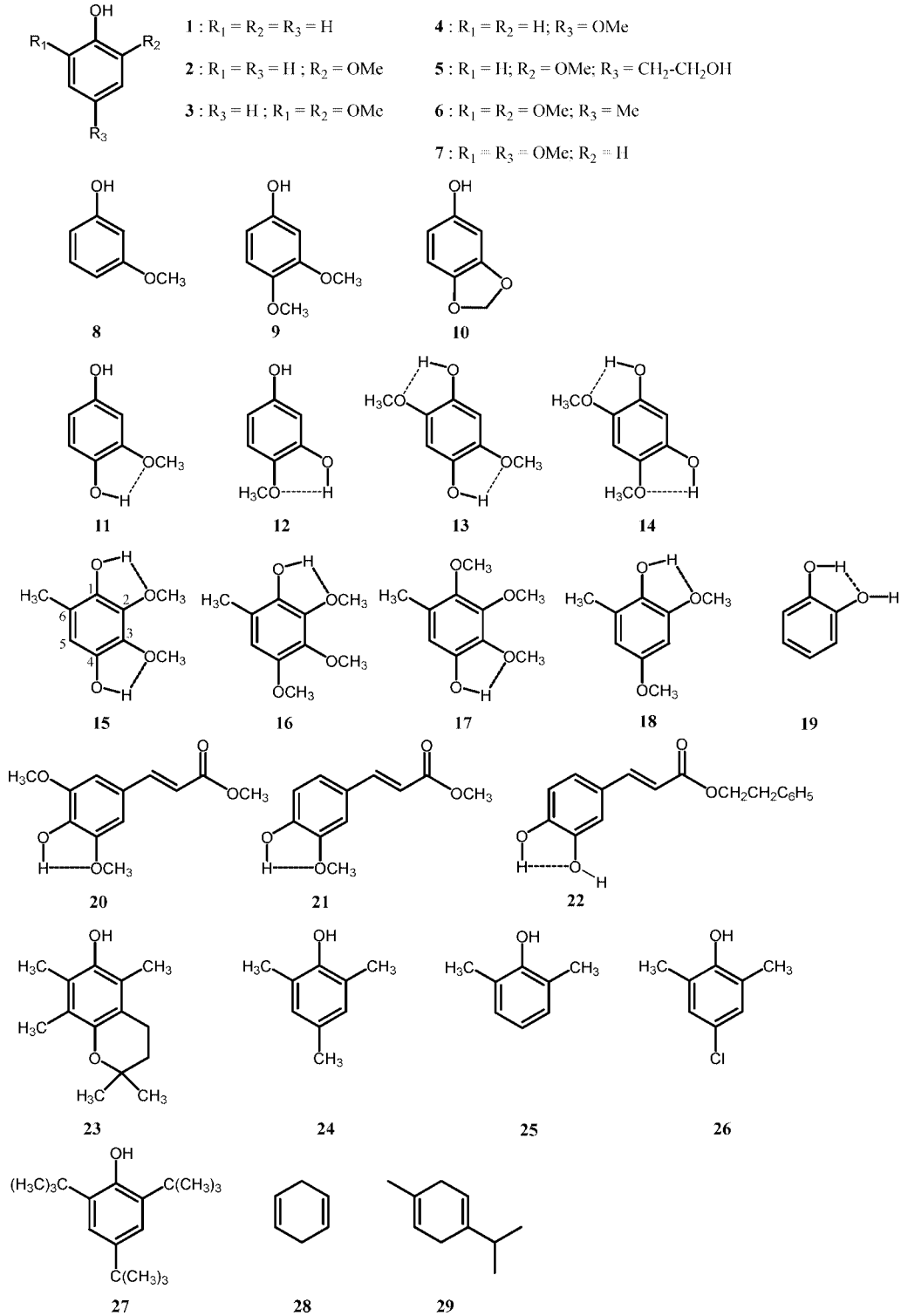

cm^{-1}. Conventional UV−vis spectroscopy was used to monitor the rates of phenol + **dpph**$^{\bullet}$ reactions at several temperatures from 5 to 70 °C using a thermostatted (±0.2 °C) stopped-flow spectrophotometer. In most cases, the solvent was neat cyclohexane or *n*-hexane but for a few phenols a small amount of ethyl acetate or CH_2Cl_2 (<2% by volume in the final solution) was added to facilit+ate dissolution and, for solubility reasons, for two phenols the solvent had to be neat methylene chloride. All solutions were purged with N_2 prior to kinetic measurements. Reactant concentrations were corrected for thermal expansion of the solvent.

The concentration of **dpph**$^{\bullet}$ was generally in the range 20−100 μM. Although the phenol concentrations were larger than the **dpph**$^{\bullet}$ concentrations (often as much as 10−50 times greater) in many cases the loss of **dpph**$^{\bullet}$ did not follow first-order kinetics over the entire course of the reaction. This behavior arises because reaction 1 is reversible. It is followed by two irreversible reactions, 3 and 4:

(16) Denisov, E. T.; Khudyakov, I. V. *Chem. Rev.* **1987**, *87*, 1313–1357.
(17) Snelgrove, D. W.; Lusztyk, J.; Banks, J. T.; Mulder, P.; Ingold, K. U. *J. Am. Chem. Soc.* **2001**, *123*, 469–477.

$$ArO^{\bullet} + \mathbf{dpph}^{\bullet} \rightarrow \text{products} \quad (3)$$

$$ArO^{\bullet} + ArO^{\bullet} \rightarrow \text{dimer or disproportionation products} \quad (4)$$

The desired second-order rate constants, k_1, were determined using various strategies. In those cases where the loss of **dpph**$^{\bullet}$ followed first-order kinetics over the entire course of reaction, values of k_1 were obtained from the slope of plots of the *observed* (pseudofirst-order) rate constants vs [ArOH], $k_{obs} = k_1[ArOH] + k_0$. In all other cases, values of k_1 were determined either from the initial rate of loss of **dpph**$^{\bullet}$ or by kinetic modeling. Modeling involved the fitting of simulated curves of **dpph**$^{\bullet}$ loss, calculated using reactions 1, 3, and 4, to the experimental curves over the entire course of the reaction. These simulations were done with the following assumptions: (i) The value of the rate constant, k_3, was $\leq A_1$ (the *A*-factor[5a] of reaction 1). (ii) $k_4 \approx 10^8-10^9$ M^{-1} s^{-1} (in most cases).[16] (iii) In a few cases, it was necessary to introduce into the modeling scheme the slow dissociation of the C−C or C−O phenoxyl radical dimer, i.e., the reverse of reaction 4, typically $k_{-4} < 50$ s^{-1}.[16] Modeling provided optimized values of the rate constants, k_1 and k_{-1}.

The poor solubility of phenols **13** and **22** in cyclohexane and *n*-hexane necessitated measurement of the kinetics in *neat* CH_2Cl_2. In these two systems, the absolute concentrations of the phenols were comparatively low, ca. 200 μM (though still higher than [**dpph**$^{\bullet}$]). The measured second-order rate constants in CH_2Cl_2 at 298 K, $k_1^{CH_2Cl_2}$, were 3000 ± 18 and 297 ± 8 M^{-1} s^{-1} for **13** and **22**, respectively. Since CH_2Cl_2 is a hydrogen bond acceptor (HBA), these two k_1 values will be lower than in a (non-HBA) saturated hydrocarbon,[11,17] and therefore, they are not directly comparable with the k_1 values for the other phenols. Fortunately, the magnitude of the CH_2Cl_2-induced rate reduction for each phenol will be the same whether reaction 1 occurs primarily by the HAT or by the PCET mechanism.[11] The rate reductions arise because only that (small) fraction of phenol molecules that are not hydrogen bonded to a CH_2Cl_2 molecule can react with an attacking **dpph**$^{\bullet}$ radical.[11,17] The required room temperature rate constant in an alkane solvent, k_1, can be reliably calculated from the measured room temperature rate constant, k_1^S, in a neat HBA solvent, S, via eq I.[11,17]

$$\log k_1 = \log k_1^S + 8.3\alpha_2^H\beta_2^H \quad (I)$$

In this equation, α_2^H and β_2^H quantify the hydrogen-bond donor (HBD) activity of the phenol reactant[18] and the HBA activity of S,[19] respectively. From the 298 K rate constants for the reaction of **dpph**$^{\bullet}$ with catechol **19** ($\alpha_2^H = 0.726$)[20] in cyclohexane (1900 M^{-1} s^{-1}) and in CH_2Cl_2 (85 M^{-1} s^{-1}), the most appropriate value of β_2^H for CH_2Cl_2 was calculated (eq I) to be ca. 0.2. The α_2^H values of **13** and **22** have not been reported. An $\alpha_2^H \approx 0.3$ was estimated for **13** from the value for 2-methoxyphenol ($\alpha_2^H = 0.24-0.26$)[20] with the inclusion of a statistical factor of 2. An $\alpha_2^H \approx 0.7$ was estimated for **22** because such a value is intermediate between the values for catechol ($\alpha_2^H = 0.726$)[20] and 3,5-di-*tert*-butylcatechol ($\alpha_2^H = 0.67$).[20] On the basis of these estimates of α_2^H and β_2^H, the k_1 values for **13** and **22** were calculated to be ∼9400 and ∼4300 M^{-1} s^{-1}, respectively, in an alkane solvent.

Rate constants, k_1, determined as indicated above, for the reaction of **dpph**$^{\bullet}$ with phenols **1**−**27** and hydrocarbons **28** and **29** at 25 °C in an alkane solvent are given in Table 1. The temperature dependence of k_1 was determined in cyclohexane from 5 to 70 °C. All Arrhenius plots showed good linearity ($r^2 > 0.98$). The derived pre-exponential factors, A_1, and activation energies, E_{a1}, are included in Table 1. These two parameters yield the enthalpy and entropy of activation via eqs II and III[21]

$$\Delta H_1^{\ddagger} = E_{a,1} - RT \quad (II)$$

$$\Delta S_1^{\ddagger} = R[\ln A_1 + \ln(h/k_B T) - 1] \quad (III)$$

where the temperature to be used is the midpoint of the experimental range, i.e., $T \approx 310$ K; $RT \approx 0.62$ kcal/mol.

Deuterium Kinetic Isotope Effects. Cyclohexane solutions containing **dpph**$^{\bullet}$ together with phenols **1**, **2**, **3**, **9** (the solution of **9** also contained <2% by volume of CH_2Cl_2), **10**, and **23** were shaken with a few drops of D_2O. Complete deuterium exchange occured within a few minutes.[23] The clear solutions were used to determine k_1(D) values at ∼298 K. Values of k_1(H) were also obtained using similar solutions containing a few drops of H_2O. The ratios, $k_1(H)/k_1(D)$, are given in Table 2.

Theoretical Calculations.[24]

The dpph$^{\bullet}$ **Radical.** The energy-optimized[25−27] structure of **dpph**$^{\bullet}$ is shown in Figure 1, and its Cartesian coordinates are provided in the Supporting Information (SI). The steric crowding in **dpph**$^{\bullet}$ is evident from parts a and b of Figure 1: an *ortho*-hydrogen atom on each of the two phenyl groups shield the formal N$^{\bullet}$ radical center (hereafter, simply N$^{\bullet}$) from above and below the C−N$^{\bullet}$−N plane [R(N$^{\bullet}$−HC)=2.73, 2.50 Å], and a nitro group hinders access to the N$^{\bullet}$ lone pair [R(ONO−N$^{\bullet}$)= 2.77 Å]. This shielding is crucially important for the reactivity and stability of **dpph**$^{\bullet}$ because it prevents direct access to the unsatisfied valence of N$^{\bullet}$. Figure 1b shows the singly occupied molecular orbital (SOMO) of **dpph**$^{\bullet}$. The iso-surface shows that while much of the unpaired electron is shared between the two N atoms, the spin is also well-delocalized into the ring moieties.

Bond Dissociation Enthalpies of Substituted Phenols. Density functional theory (DFT)-based approaches are able to

(18) Abraham, M. H.; Grellier, P. L.; Prior, D. V.; Duce, P. P.; Morris, J. J.; Taylor, P. J. *J. Chem. Soc., Perkin Trans. 2* **1989**, 699–711.
(19) Abraham, M. H.; Grellier, P. L.; Prior, D. V.; Morris, J. J.; Taylor, P. J. *J. Chem. Soc., Perkin Trans. 2* **1990**, 521–529.
(20) Foti, M. C.; Barclay, L. R. C.; Ingold, K. U. *J. Am. Chem. Soc.* **2002**, *124*, 12881–12888.
(21) Moore, J. W.; Pearson, R. G. *Kinetics and Mechanism*, 3rd ed.; Wiley: New York, 1981.
(22) (a) Mulder, P.; Korth, H.-G.; Pratt, D. A.; DiLabio, G. A; Valgimigli, L.; Pedulli, G. F.; Ingold, K. U *J. Phys. Chem. A* **2005**, *109*, 2647–2655. (b) Brigati, G.; Lucarini, M.; Mugnaini, V.; Pedulli, G. F. *J. Org. Chem.* **2002**, *67*, 4828–4832. (c) Lucarini, M.; Pedulli, G. F.; Guerra, M. *Chem.−Eur. J.* **2004**, *10*, 933–939. (d) Wayner, D. D. M.; Lusztyk, J. E.; Page, D.; Ingold, K. U.; Mulder, P.; Laarhoven, L. J. J.; Aldrich, H. S. *J. Am. Chem. Soc.* **1995**, *117*, 8737–8744. (e) Wayner, D. D. M.; Lusztyk, J.; Ingold, K. U.; Mulder, P. *J. Org. Chem.* **1996**, *61*, 6430–6433.
(23) See, e.g.: Gardner, D. V.; Howard, J. A.; Ingold, K. U. *Can. J. Chem.* **1964**, *42*, 2847–2851, and references cited therein.
(24) All calculations were performed using: Gaussian 03, Revision C.02: Frisch, M. J.; Trucks, G. W.; Schlegel, H. B.; Scuseria, G. E.; Robb, M. A.; Cheeseman, J. R.; Montgomery, J. A., Jr.; Vreven, T.; Kudin, K. N.; Burant, J. C.; Millam, J. M.; Iyengar, S. S.; Tomasi, J.; Barone, V.; Mennucci, B.; Cossi, M.; Scalmani, G.; Rega, N.; Petersson, G. A.; Nakatsuji, H.; Hada, M.; Ehara, M.; Toyota, K.; Fukuda, R.; Hasegawa, J.; Ishida, M.; Nakajima, T.; Honda, Y.; Kitao, O.; Nakai, H.; Klene, M.; Li, X.; Knox, J. E.; Hratchian, H. P.; Cross, J. B.; Adamo, C.; Jaramillo, J.; Gomperts, R.; Stratmann, R. E.; Yazyev, O.; Austin, A. J.; Cammi, R.; Pomelli, C.; Ochterski, J. W.; Ayala, P. Y.; Morokuma, K.; Voth, G. A.; Salvador, P.; Dannenberg, J. J.; Zakrzewski, V. G.; Dapprich, S.; Daniels, A. D.; Strain, M. C.; Farkas, O.; Malick, D. K.; Rabuck, A. D.; Raghavachari, K.; Foresman, J. B.; Ortiz, J. V.; Cui, Q.; Baboul, A. G.; Clifford, S.; Cioslowski, J.; Stefanov, B. B.; Liu, G.; Liashenko, A.; Piskorz, P.; Komaromi, I.; Martin, R. L.; Fox, D. J.; Keith, T.; Al-Laham, M. A.; Peng, C. Y.; Nanayakkara, A.; Challacombe, M.; Gill, P. M. W.; Johnson, B.; Chen, W.; Wong, M. W.; Gonzalez, C.; Pople, J. A. Gaussian, Inc., Pittsburgh PA, 2003.
(25) Using B3LYP[26,27]/6-31G(d).
(26) Becke, A. D. *J. Chem. Phys.* **1993**, *98*, 5648–5652.
(27) Lee, C.; Yang, W.; Parr, R. G. *Phys. Rev. B* **1988**, *37*, 785–789.

TABLE 1. Rate Constants k_1 and k_{-1} (M^{-1} s^{-1}, 298 K), Arrhenius Parameters A_1 (M^{-1} s^{-1}), and $E_{a,1}$ (kcal/mol) for the Reactions of Phenols 1−27 and Hydrocarbons 28 and 29 with dpph• in an Alkane Solvent (Experimental/Estimated[a] ArO-H BDEs (kcal/mol) in Solution at 298 K (1 M Standard State), Error ± 1 kcal/mol, and Calculated ArO-H BDEs in the Gas Phase at 298 K (1 atm Standard State))[b]

no.	substituents	k_1[c]	k_{-1}[d]/10^4	A_1[e]/10^5	E_{a1}	OH BDE[a,b,f]	source[a]
1	none	0.10		16.0	9.8	86.3 (87.8)	22a
2	2-OMe	0.92	4	1.7	7.2	85.1 (85.5)	5a
3	2,6-di-MeO	50	1.1	2.9	4.9	82.1 (81.7)	10b
4	4-MeO	238		19.0	5.3	82.0[g] (82.2)	22e, 10b, AR
5	2-MeO-4-CH_2CH_2OH	3	3	*1.7*	6.5	83.9 (84.2)	AR
6	2,6-di-MeO-4-Me	180	0.73	*2.9*	4.4	81.0 (80.2)	AR
7	2,4-di-MeO	155		4.1	4.7	81.5 (81.1)	14
8	3-MeO	1.4	16	*16.0*	8.3	85.7 (86.6)	K
9	3,4-di-MeO	1800		6.6	3.6	80.4 (80.0)	eq *X*
10	sesamol	935		6.0	3.8	80.6 (80.6)	eq *X*
11	2-MeO-4-OH	4400		11.0	3.25	80.0 (80.2)	eq *X*
12	3-OH-4-MeO	200		12	5.1	82.1 (83.0)	eq *X*
13	2,5-di-MeO-4-OH	9400[h]		*2.3*	2.0	≤78.7[i] (79.1)	eq *X*
14	3-OH-4,6-di-MeO	999		2.3	3.2	80.0 (78.9)	eq *X*
15	ubiquinol-0	990	0.5	1.5	3.3	78.5 (78.5)	
16	ubiquinol-0 ether	68	1	1.3	4.5	82.1 (80.6)	5a
17	ubiquinol-0 ether	11	1.8	*1.5*	5.6	83.4 (82.1)	5a
18	2,4-di-MeO-6-Me	482		3.5	3.9	80.8 (79.6)	eq *X*
19	2-OH	1900		7.3	3.5	80.7 (77.2)	22c
20	sinapic acid	226	0.7	2.9	4.2	81.2 (80.7)	5a
21	ferulic acid	10	1.9	*1.7*	5.8	83.5 (84.7)	5a
22	CAPE	4300[h]		*7.3*	3.2	80.0 (75.7)	eq *X*
23	PMHC	8415		5.9	2.5	77.2 (75.3)	10b
24	2,4,6-tri-Me	47		1.6	4.85	81.6 (81.4)	10b
25	2,6-di-Me	4.3		1.7	6.3	83.4 (83.2)	10b
26	2,6-di-Me-4-Cl	5		2.0	6.2	83.0 (82.3)	AR
27	2,4,6-tri-^{t}Bu	0.91		0.045	5	80.1 (78.2)	22a
28		0.00100[l]		4.6	11.8	(74.1)	
29		0.00156[l]		4.1	11.5	(74.0)	

[a] The experimental BDEs, when available, are taken from the literature (references indicated); otherwise they have been estimated with the substituent additivity rules[5a,22b] (AR) or from $E_{a,1}$ (eq X), or from the kinetics (K) for reactions 1 and −1 (as described for **8** in the text). [b] BDEs computed by density functional theory are given in parentheses. See text for additional details. The standard states in which the reported ArO-H BDEs are obtained differ, viz. 1 M for experimental and 1 atm for calculated BDEs; to convert between the two standard states, BDE(1 atm) = BDE(1 M) + 0.4 kcal/mol at 298 K. [c] Reproducibility was better than ± 10%. [d] Values obtained by simulation (see text). [e] A factors for **5**, **6**, **8**, **17**, **20**, **21**, and **22** (given in italics) were assumed to be equal to those for **2**, **3**, **1**, **15**, **3**, **2**, and **19**, respectively. [f] The experimental OH BDEs determined via the electron paramagnetic resonance, radical buffer technique (refs 10 and 22b, c) were adjusted downward by 1.1 kcal/mol as indicated in ref 22a. [g] This is the average of two experimental values (81.3 and 81.8 kcal/mol) and an AR estimation (82.8 kcal/mol). [h] Rate constant calculated for an alkane solvent from value measured in CH_2Cl_2 (see text). [i] Reaction 1 with this phenol is likely to be thermoneutral or slightly exothermic and thus the ArO-H BDE obtained by eq X is most likely overestimated (see text). [l] Rate constant based on initial rates. The kinetics (in the absence of dioxygen) were complicated by autocatalysis (see the Experimental Section).

TABLE 2. Deuterium Kinetic Isotope Effects for Reaction *1* in Cyclohexane at ca. 298 K and Reaction Enthalpies ΔH_1 (kcal/mol)

ArOH	$k_1(H)/k_1(D)$[a]	ΔH_1^{H}[b]
phenol (**1**)	2.0	7.4
2-methoxyphenol (**2**)	3.3	6.2
2,6-dimethoxyphenol (**3**)	3.3	3.2
3,4-dimethoxyphenol (**9**)	1.4	1.1
sesamol (**10**)	1.3	1.6
PMHC (**23**)	1.9	−1.7

[a] These ratios are the average of three different measurements. The relative error is estimated to be approximately ± 20%. [b] The N-H BDE of **dpph**-H is 78.9 ± 0.5 kcal/mol (see ref 5a).

compute reasonably accurate BDEs in many cases. In this work, we have calculated the O−H BDEs for the phenols listed in Table 1 using a DFT-based approach outlined previously by one of us.[28] The method works quite well for many applications but, like most other DFT methods, is subject to deficiencies related to improper modeling of van der Waals interactions and overstabilization from electron delocalization. Nevertheless, the DFT-calculated O-H BDEs are in very good agreement with those determined by EPR and other methods. The absolute value computed for the PhO-H BDE is 87.8 kcal/mol, which is in good agreement with the critically evaluated "best" value of 86.7 ± 0.7 kcal/mol.[22a] The average deviation between the calculated and experimental O-H BDEs in Table 1 is ca. 1 kcal/mol. Note that the estimated error on the measured BDEs is ± 1 kcal/mol. A similarly good result is obtained for the N-H BDE of **dpph**-H, viz. calculated 79.6 kcal/mol vs measured 78.9 ± 0.5 kcal/mol.[5a]

The largest errors in the calculated BDEs are associated with catechol **19** and caffeic acid phenethyl ester (CAPE), **22**, for which the O−H BDEs are computed to be, respectively, 3.5 and 4.3 kcal/mol lower than the measured values. A careful examination of the molecule and radical stabilization enthalpies[30] for these two systems reveals that the computed increase in the strength of the intramolecular HB on going from the phenol to the phenoxyl radical has probably been overestimated. This overestimation is probably connected with the well-known "delocalization problem" in DFT[31] because many of the different functionals we used to explore this problem also gave O-H

(28) Using the approach outlined in: Johnson, E. R.; Clarkin, O. J.; DiLabio, G. A *J. Phys. Chem. A* **2003**, *46*, 9953–9963, which is based on the B3[26]P86[29] method.

(29) Perdew, J. P. *Phys. Rev. B* **1986**, *33*, 8822–882X.

(30) Pratt, D. A.; DiLabio, G. A.; Mulder, P.; Ingold, K. U. *Acc. Chem. Res.* **2004**, *37*, 334–340.

(31) Johnson, E. R.; Becke, A. D. *J. Chem. Phys.* **2008**, *128*, 124105.

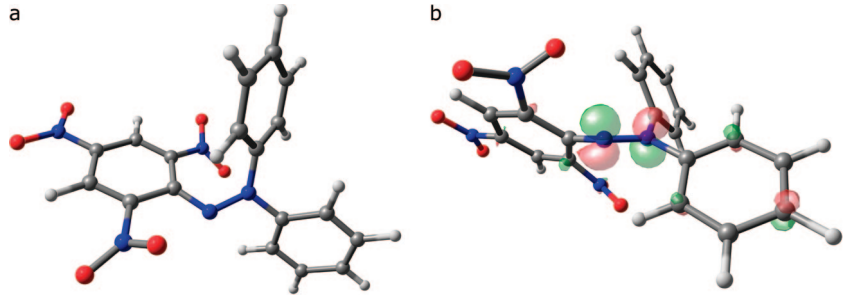

FIGURE 1. Perspective images of the calculated structure of **dpph•**. The constituent atoms are colored as follows: oxygen = red, nitrogen = blue, carbon = gray, hydrogen = white. (a) The view is approximately perpendicular to the plane defined by the hydrazyl group N atoms and the C1 of the picryl ring. (b) The view is approximately in the plane defined by the hydrazyl group N atoms and the C1 of the picryl ring. The singly occupied molecular orbital (SOMO) is also shown, with the red and green colors representing the two phases of the orbital.

BDEs in **19** and **22** that were lower than the experimental values. We note that the O-H BDEs obtained from the DFT treatment of molecules (not *both* molecules and radicals) containing intramolecular HBs, for example, **2**, **12**−**18**, **20**, and **21**, are in rather good agreement with experiment.

The O-H BDEs in catechol (and probably all substituted phenols) can be calculated accurately using the coupled cluster with single and double excitations (CCSD) correlated wave function approach, with correlation consistent basis sets and with basis set extrapolation.[32] This is the case because the CCSD method does not suffer from the delocalization problems that plague most DFT methods. Unfortunately, calculations of this type are extremely time-consuming. However, we have previously shown that a locally dense basis set (LDBS) approach can be used to reduce the computational requirements associated with such calculations.[33] In the LDBS approach, regions of chemical importance within a molecule or radical are treated using larger basis sets and regions of lesser chemical importance are treated using smaller basis sets.[34] This LDBS technique gives an O-H BDE for phenol of 87.2 kcal/mol,[35] in excellent agreement with the measured value given in Table 1 and with the "best" value of 86.7 ± 0.7 kcal/mol. [22a] The CCSD/LDBS O-H BDE for catechol is 80.3 kcal/mol, which is 6.9 kcal/mol less than phenol. This ΔBDE value is in excellent accord with our previous assessment of 7.0 ± 0.2 kcal/mol[36] and, within the error bars, of the experimental ΔBDE value of 5.6 kcal/mol obtained from Table 1.[37]

Hydrogen Bonding to dpph. Additional calculations were performed on a few conformations of HB complexes between **dpph•** and *p*-methoxyphenol[38] in order to provide some insight into the nature of **dpph•**/ArOH prereaction complexes. An exhaustive search of conformational space was not performed. However, some important structures were obtained, and a selection of these are collected in the Supporting Information. The calculations support our expectations that the three NO_2 groups of **dpph•** are stronger HB acceptors than the lone-pair on N•.

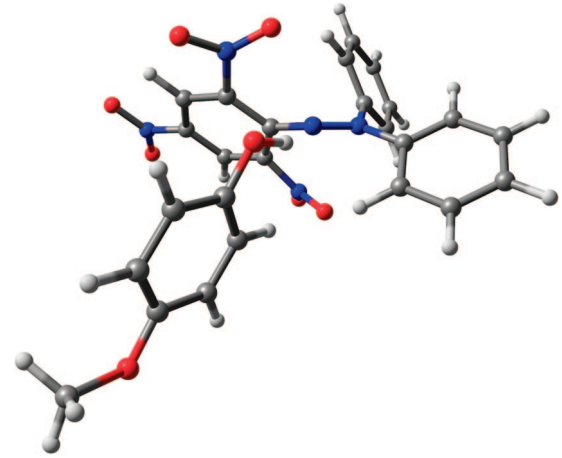

FIGURE 2. Structure of the HB complex of **dpph•** and *p*-methoxyphenol to the N• lone pair. This is the prereaction complex formed prior to H atom transfer from the phenol to **dpph•**. The deviation of the H-bond from linearity, defined by θ(O−H−N•), is ca. 26.3°. The extent to which the nascent transferring H atom deviates from residing in the plane defined by the picryl C1 and the hydrazyl N atoms, φ(H−C−N•−N), is 12.6°. See the Supporting Information for additional details.

For the prereaction complex (see Figure 2), the calculations predict that the OH group of the phenol remains essentially in the plane of the phenol's ring upon HB formation, viz., φ(H−O−C−C) = 6.3°. The HB angle, θ(O−H−N•), deviates from the ideal value of 180° by 26.3 because of steric effects. The extent to which the nascent transferring H atom deviates from being in the plane defined by the picryl C1 and the hydrazyl N atoms, i.e. φ(H−C−N•−N), is 12.6°. Also, the phenolic ring is, for steric reasons, oriented roughly perpendicular to the plane defined by C−N•−N.[39] Similar geometric parameters were found for prereaction complexes involving **1** and **8** (see the Supporting Information).

It is very important to point out that we were unable to obtain a reasonable, bound structure involving HB formation with the

(32) We used the basis set extrapolation method suggested in: Martin, J. M. L. *Chem. Phys. Lett.* **1996**, *259*, 669–678.

(33) See, for example: DiLabio, G. A. *J. Phys. Chem. A* **1999**, *51*, 11414–11424. Johnson, E. R.; McKay, D. J. J.; DiLabio, G. A. *Chem. Phys. Lett.* **2007**, *435*, 201–207.

(34) In this work, LDBS calculations of the O-H BDEs in phenol and catechol, viz. C_6H_5**OH** → C_6H_5**O•** + **H•** and C_6H_4**OHOH** → C_6H_4**OHO•** + **H•**, used aug-cc-pVDZ and aug-cc-pVTZ basis sets on the bold atoms and cc-pVDZ basis sets on the remaining atoms.

(35) We note that these calculations are not thorough with respect to basis set size, basis set extrapolation, or electron correlation. However, more extensive treatments may not yield results in better agreement with the best available experimental O−H BDE data. This is exemplified to some extent in: Costa Cabral, B. J.; Canuto, S. *Chem. Phys. Lett.* **2005**, *406*, 300–305, and commented upon in ref 36.

(36) DiLabio, G. A.; Mulder, P. *Chem. Phys. Lett.* **2006**, *417*, 566–569.

(37) It is worthwhile pointing out that these calculations can be further simplified by using extrapolated MP4(SDQ) energies to correct the CCSD/aug-cc-pVDZ LDBS energies. Additional information is provided in the Supporting Information.

(38) Using B3LYP/6-311++G(2d,2p)//B3LYP/6-31G(d) as implemented in ref 24.

(39) For reference, the "*ideal*" PCET (HAT) pre-reaction complex structure would have θ(O−H−N•) = 180° (180°), φ(H−O−C−C) = 0° (90°), and φ(H−C−N•−N) = 0° (90°), and the phenolic ring co-planar with (perpendicular to) the C−N•−N plane.

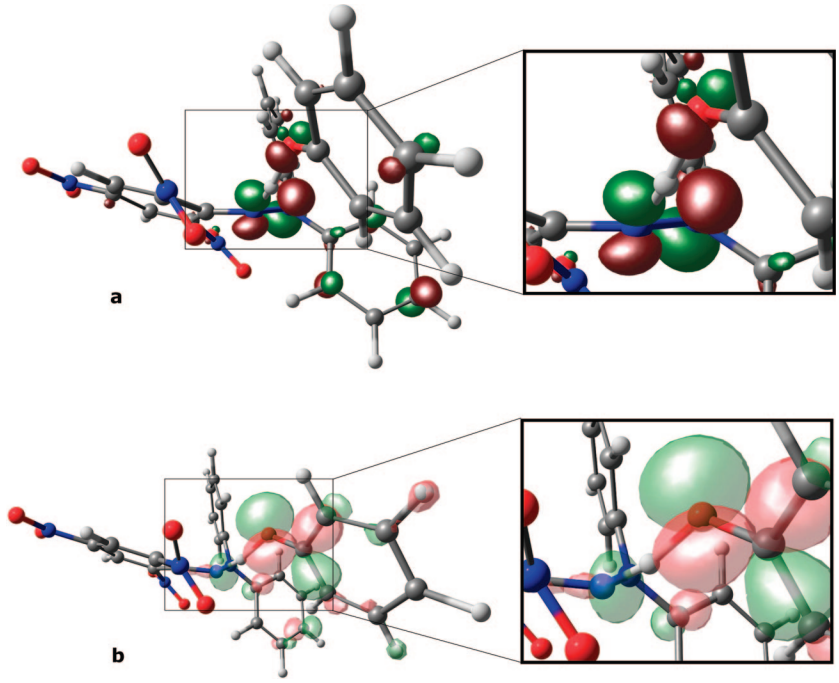

FIGURE 3. Calculated transition state structures for hydrogen atom exchange between phenol and **dpph•**. The view is in the C−N•−N plane with the phenol ring in the foreground. The constituent atoms are colored as follows: oxygen = red, nitrogen = blue, carbon = gray, hydrogen = white. To help guide the eye, bonds between the O, H, and N atoms involved in the H-transfer have been drawn. Key structural information associated with the atoms at the atom transfer center are given below. The degree to which the OH group is rotated out of the plane of the phenol ring is indicated by φ(H−O−C−C) and the extent to which the transferring H-atom deviates from coplanarity with the picryl C1 and the hydrazyl N atoms is indicated by φ(H−C−N•-N). For phenol, (**1**), TS: R(O−H) = 1.25 Å, R(H−N•) = 1.22 Å, θ(O−H−N•) = 161.7°, φ(H−O−C-C)= 43.8°, φ(H−C−N•−N)= 40.1°. Related TS structures not shown in this figure: *m*-methoxyphenol, **8**, R(O−H) = 1.23 Å, R(H−N•) = 1.24 Å, θ(O−H−N•) = 162.9°, φ(H−O−C−C)= 44.4°, φ(H−C−N•−N)= 39.6°. *p*-Methoxyphenol, **4**, R(O−H) = 1.19 Å, R(H−N•) = 1.22 Å, θ(O−H−N•) = 163.9°, φ(H−O−C−C)= 40.9°, φ(H−C−N•−N)= 38.8°. TS molecular orbitals, with relative phases indicated by the red and green colors: (a) Singly occupied molecular orbital (SOMO). The nominally singly occupied p-type orbital on N• is particularly evident in the magnified view. The component of the orbital on **dpph•** is very similar to the SOMO on isolated **dpph•**; see Figure 1b. (b) A low-energy, doubly occupied molecular orbital (HOMO-6) showing the lone-pair orbital on N•.

unpaired electron on the N• in **dpph•**. *The formation of a prereaction complex that would favor direct hydrogen atom transfer from the OH group of a phenol to the orbital on the hydrazyl moiety of* **dpph•** *that holds the unpaired electron would appear to be highly disfavored.*

Transition-State Structures and Kinetics for the Reaction of dpph• with Three Phenols. The calculated[40] transition-state (TS) structure for the reaction of **dpph•** with **1** is shown in Figure 3 along with some structural parameters for the TSs involving **1**, **4**, and **8**. For each of these reactions, only a single TS structure was explored. It is expected that other, higher energy pathways are also possible for these reactions. Kinetic parameters associated with the reactions were obtained from transition-state theory in a manner described previously and incorporate quantum-mechanical tunnelling.[12b]

The trends of the O−H bond lengths in the TS structures involving **1**, **8**, and **4** (see Figure 3 caption) follow that which is expected based on the O−H BDEs of the corresponding phenols, viz. **1** > **8** > **4**, see also Table 1. Steric hindrance causes θ(O−H−N•) in the TSs to be ca. 16 to 18° away from linearity,[39] as it does in the H-bonded prereaction complexes, see Figure 2. To some extent, steric hindrance in the TS is responsible for φ(H−O−C−C) dihedral angles that are 40.9 − 44.4° ("ideal" 0° for PCET, 90° for HAT).[39] Interestingly, values of φ(H−C−N•−N), for which the "ideal" value is 0° for PCET and 90° for HAT,[39] track the O−H BDE values in the phenols, viz. **1** (40.1°) > **8** (39.6°) > **4** (38.8°). Thus, in H-atom exchange between phenols and **dpph•** the TS structures deviate considerably from the "ideal" PCET geometry that would presumably be obtained in the absence of steric hindrance.[39]

Figure 3 also displays the singly occupied molecular orbital (SOMO) and a low-lying doubly occupied molecular orbital (six orbitals below highest-occupied molecular orbital (HOMO), i.e. HOMO-6) for the TS structure of the reaction of **1** with **dpph•**, which are representative of the orbitals of TSs involving other phenols. A fuller appreciation of the structure of the orbitals shown in Figure 3 can be obtained by viewing the animations given in the SI. The orbitals reveal that the transferring H atom interacts with both the singly occupied p-type orbital on N• (see magnified area in Figure 3a) and with the lone-pair orbital on the N• (see magnified area in Figure 3b).

The calculated $E_{a,1}$ values[40] associated with the reactions of **1**, **4**, and **8** are in very good agreement with those obtained from experiment (see Table 1), viz. calculated (experimental)

(40) The calculations involved the use of the LDBS approach in conjunction with the B3LYP DFT method for structure optimizations. Additional details of the LDBS partitioning are given in the Supporting Information. TSs were optimized and validated by animating the single negative vibration mode that connects reactants to products. Following the geometry optimizations, we performed single-point energy calculations at the B3LYP/6-311++G(2d,2p) level of theory. We used this approach to study HAT/PCET in some prototypical systems in reference 12b. However, in the present work, B3LYP tends to give $E_{a,1}$ values that are too large, likely because the TS structures are very sterically crowded. We found better agreement between calculated and experimental $E_{a,1}$ values in this work by computing single-point energies with B971/6-311++G(2d,2p). The better agreement is most like due to the fact that B971 can, to some extent, predict dispersion binding in some systems.[41]

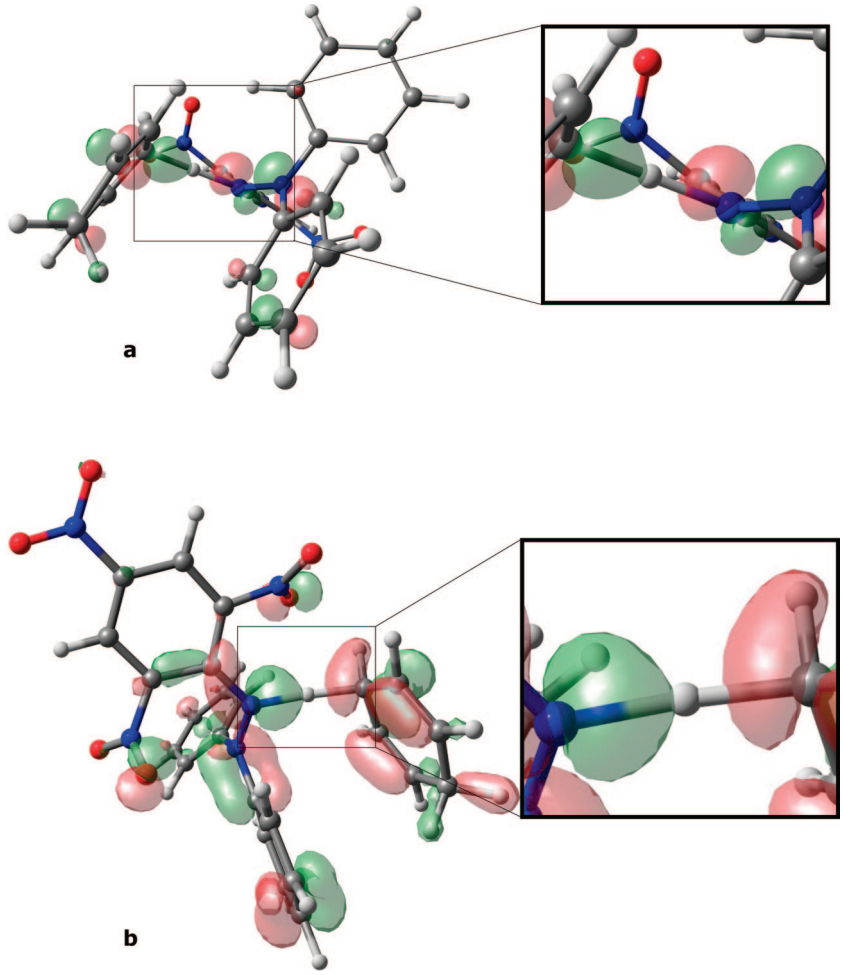

FIGURE 4. Calculated transition state structure for hydrogen atom exchange between 1,4-cyclohexadiene and **dpph•**. The view is in the C−N•−N plane with one phenyl ring of the **dpph•** in the foreground on the right. The constituent atoms are colored as follows: oxygen = red, nitrogen = blue, carbon = gray, hydrogen = white. To help guide the eye, bonds between the O, H, and N atoms involved in the H transfer are drawn in. Key structural information associated with the atoms at the atom transfer center are as follows: R(HC−H) = 1.35 Å, R(H−N•) = 1.36 Å, θ(HC−H−N•) = 175.7°. The extent to which the transferring H atom deviates from coplanarity with the picryl C1 and the hydrazyl N atoms, φ(H−C−N•−N), is 22.8°. TS molecular orbitals, with relative phases indicated by the red and green colors: (a) Singly occupied molecular orbital (SOMO) showing the nominally singly occupied p-type orbital on N•. The component of the orbital on **dpph•** is very similar to the SOMO on isolated **dpph•**; see Figure 1b. (b) A low energy, doubly occupied molecular orbital (HOMO-8) showing the lone-pair orbital on N•.

$E_{a,1}$(**1**) = 9.5 (9.8), $E_{a,1}$ (**4**) = 4.7 (5.3), and $E_{a,1}$ (**8**) = 8.3 (8.3) kcal/mol.[42] The calculated rate constants, k_1, are also in reasonably good agreement with measured values (see Table 1), viz. calculated (experimental) k_1(**1**) = 0.44 (0.10), k_1(**4**) = 730 (238), and k_1(**8**) = 17.0 (1.4) M^{-1} s^{-1} at 298 K and maintain the correct trend. The calculated Arrhenius pre-exponential factors, A_1(**1**) = 25, A_1(**4**) = 30, and A_1(**8**) = 130 × 10^5 M^{-1} s^{-1} at 298 K are in less satisfactory agreement with the experimental values of (16−19) × 10^5 M^{-1} s^{-1}; see Table 1.

The calculated TS structure for the reaction of 1,4-cyclohexadiene, **28**, with **dpph•** is shown in Figure 4, and its structural parameters are given in the figure caption. There are important differences between the TS structure shown in Figure 4 and the TS structures involving phenols. Specifically, the bond lengths at the TS center are ca. 0.1 Å longer than those in phenols, and the cyclohexadiene molecular plane is oriented perpendicular to the direction of H atom transfer. In addition, the out-of-plane angle, φ(CH−C−N•−N), is 22.8°, much closer to the "ideal" value of 0° for PCET[39] than the analogous dihedral angles in the phenols.

Figure 4 also displays the SOMO and a low-lying doubly occupied molecular orbital (HOMO-8) for the TS structure of the reaction of **28** with **dpph•**. Animations of the orbitals are also provided in the SI. As is the case for the phenol + **dpph•** TS, the orbitals show that the transferring H atom interacts with both the singly occupied p-type orbital on N• (see magnified area in Figure 4a) and with the lone-pair orbital on the N• (see magnified area in Figure 4b).

The kinetic parameters calculated for the reaction of 1,4-cyclohexadiene with **dpph•** are in very poor agreement with the measured values presented in Table 1. For example, E_a is calculated to be 19.8 kcal/mol which is more than 8 kcal/mol higher than the experimental value. A goodly portion of this discrepancy can probably be attributed to the dispersion problem

(41) There are a large number of papers on this general subject. One of our recent works in this area compares the binding in van der Waals complexes as calculated by several DFT methods to that obtained by second-order Møller−Plesset perturbation theory (MP2, a low-level, correlated wavefunction method). See: Johnson, E. R.; DiLabio, G. A. *Chem. Phys. Lett.* **2006**, *419*, 333–339.

(42) Analogous data obtained using B3LYP/6-311++G(2d,2p) overestimate $E_{a,1}$ by 1.8 to 2.3 kcal/mol but the trends of the calculated values nicely follow that established by the measured $E_{a,1}$ and O-H BDE. The discrepancies between the B3LYP-calculated and measured $E_{a,1}$'s are partially due to the fact that B3LYP, as most DFT methods, overestimates steric repulsion.[41]

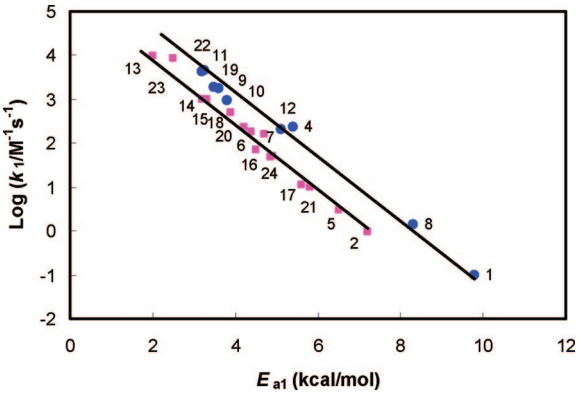

FIGURE 5. Plots of log k_1/M^{-1} s^{-1} at 298 K vs E_{a1} for nine phenols with "free" OH groups (blue circles) and for ten phenols with an intramolecular H-bonded OH group plus four 2,6-dimethylphenols (both as red squares): the slopes of the best-fitted straight-lines were set equal to their theoretical value of $1/2.303RT = 0.733$ mol/kcal while the intercepts were left to float: log $k_1 = 6.080 - 0.733E_{a1}$ ($r^2 = 0.986$) and log $k_1 = 5.342 - 0.733E_{a1}$ ($r^2 = 0.975$), respectively. The intercepts yield, as the most representative A_1 values for these two groups of phenols, $(1.2 \pm 0.5) \times 10^6$ and $(2.2 \pm 0.8) \times 10^5$ M^{-1} s^{-1}, respectively.

in DFT which is likely to be particularly bad because the "face-on" orientation of the 1,4-cyclohexadiene (in contrast to the "edge-on" orientation of phenols) will involve strong steric repulsions with the ring moieties of **dpph•**.

Discussion

Kinetics and Mechanism of Reaction of Phenols with the dpph• Radical. Table 1 shows that the *A*-factors for phenols with both *ortho*-positions free are higher than the *A*-factors for phenols having substituents at the *ortho*-positions. The lowest value, 4.5×10^3 M^{-1} s^{-1}, was measured for 2,4,6-tri-*tert*-butylphenol, **27**, and corresponds to an activation entropy of −43.9 cal/mol•K. The highest value, 1.9×10^6 M^{-1} s^{-1}, was found with 4-methoxyphenol, **4**, and corresponds to $\Delta S_1^{\ddagger} = -31.9$ cal/mol•K. The *A*-factors for phenols with "free" OH's are scattered around 1.2×10^6 M^{-1} s^{-1} ($\Delta S_1^{\ddagger} = -32.9$ cal/mol•K), whereas for intramolecularly hydrogen-bonded and 2,6-dimethylphenols the *A*-factors are around 2.2×10^5 M^{-1} s^{-1} ($\Delta S_1^{\ddagger} = -36.1$ cal/mol•K), see Figure 5. These two A-factor domains, and the even smaller A_1 factor for **27**, demonstrate that the activation entropy and, hence, the probability of H-atom transfer, decreases substantially with increasing steric protection of the phenol's OH group. Indeed, the A_1 factors are sufficiently distinct between phenols with "free" OH's and phenols with an OH that forms an intramolecular HB or lies between two methyl groups that the reactive OH group in polyphenols can often be identified. For example, **11** and **12** have "high" A_1 values, implying that their more reactive OH's are those that are not hydrogen bonded.

By using eqs II and III and the values of $E_{a,1}$ and A_1 from Table 1, it can be shown that the entropic contribution to the free energy barrier to reaction is greater than the enthalpic contribution, i.e., $-T\Delta S_1^{\ddagger} > \Delta H_1^{\ddagger}$. Indeed, entropy can contribute more than 70% to the free energy barrier. Nevertheless, and despite the fact that $\Delta H_1^{\ddagger}$ accounts for only about 30% of the barrier, Figure 5 demonstrates that, for a family of phenols with no (or with rather similar) steric protection of their OH groups, the rate constants for reaction 1 are under enthalpic control. Indeed, for the phenols with "free" OH groups, k_1 values vary by about 5 orders of magnitude in response to variations in $E_{a,1}$ as a consequence of the effects of the ring substituents.

Our DFT calculations indicate that the reaction of phenols with **dpph•** must occur by one pathway and via a single TS structure. The mechanism for these reactions cannot be described as either PCET or HAT, but as some combination of the two.[43] This is consistent with the results of our previous computational studies on prototypical H-atom exchange reactions.[12b] The geometries and the nature of the HOMOs and SOMOs of the TS structure are not "ideal" for PCET or for HAT, see Figure 3. The phenolic proton may be transferred to the lone pair on the N• of the **dpph•** radical with the accompanying electron presumably coming from a lone pair on the phenolic oxygen atom (i.e., PCET). However, the good orbital overlaps required to allow facile electron transfer appear to be absent. Similarly, the phenolic proton may also be transferred with one of its bonding electrons to the unpaired electron on the N• of the **dpph•** (i.e., HAT), but both the nuclear and electronic structures of the TSs are far from ideal for this to be the dominant mechanism.

The *A*-factors for phenols are significantly lower than the "normal" *A*-factor for a bimolecular H-atom transfer, evaluated to be $\sim 10^{8.5\pm0.5}$ M^{-1} s^{-1}.[8] Since the N• of **dpph•** is sterically very well shielded, the entropy requirements in approaching the TS structure are expected to be particularly unfavorable. This must be the main cause of the observed low A-factors. The *A*-factors for reaction of **dpph•** with the two 1,4-cyclohexadienes, **28** and **29**, are 4.6×10^5 and 4.1×10^5 M^{-1} s^{-1}, respectively (Table 1), which are even smaller than the *A*-factors for phenols with "free" OH groups. For these two hydrocarbons, no HB formation can occur (though there might be some weakly held, dispersion-bound complexes or nonreactive charge-transfer complexes). The small *A*-factors for **28** and **29** must be due, primarily, to steric hindrance to reaction. In this connection, the *A*-factors for H-atom transfers between two oxygen atoms, reaction 5, rather than between oxygen and nitrogen, reaction 1,

$$YO^{\bullet} + XOH \rightarrow YOH + XO^{\bullet} \qquad (5)$$

decrease dramatically with increased steric protection of the reactive sites.[45] For example, for $YO^{\bullet} = Me_3COO^{\bullet}$, $A = 10^{7.2}$ M^{-1} s^{-1}, $E_a = 5.2$ kcal/mol for XOH = phenol,[46] but for XOH = 2,6-di-*tert*-butyl-4-methylphenol *A* is only $10^{4.6}$ M^{-1} s^{-1} and $E_a = 0.8$ kcal/mol.[47] These results show that steric hindrance to H-atom transfers can result in an unfavorable activation entropy rather than an unfavorable activation enthalpy (as is commonly supposed). There is no reason to

(43) Katarina[44] has used a lower level of theory to deduce the mechanisms of the reactions of a number of phenols with **dpph•**. The distinction between the HAT and PCET processes was made on the basis of the difference in the transferred H-atom's charge in the TS relative to the starting phenol. A decrease in this charge in the TS was taken to indicate that the HAT pathway was dominant, while an increase in charge in the TS was taken to indicate a dominant PCET mechanism. However, the mechanistic choices that were made on this basis are difficult to accept. Phenols with quite similar structures, some with electron-donating and others with electron-withdrawing substituents were put in the HAT category while others were put in the PCET category. For example, the HAT mechanism was deduced for phenol, 4-*tert*-butylphenol, 2-methoxyphenol, and 4-dimethylaminophenol, but the PCET mechanism was proposed for 4-methylphenol, 4-methoxyphenol, and 4-chlorophenol, see Table 3 in ref 44.

(44) Katarina, N. M. *THEOCHEM* **2007**, *818*, 141–150.

(45) For a summary, see: DiLabio, G. A.; Ingold, K. U. *J. Am. Chem. Soc.* **2005**, *127*, 6693–6699.

(46) Chenier, J. H. B.; Furimsky, E.; Howard, J. A. *Can. J. Chem.* **1974**, *52*, 3682–3688.

(47) Howard, J. A.; Furimsky, E. *Can. J. Chem.* **1973**, *51*, 3738–3745.

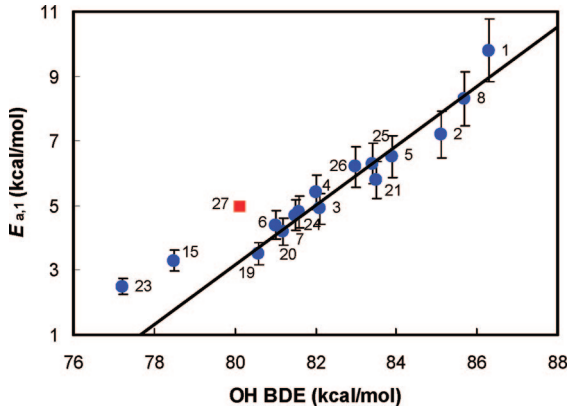

FIGURE 6. Plot of activation energy for reaction 1 vs ArO-H BDE for those phenols shown in Chart 1 for which reliable BDEs were available (see Table 1). Blue circles are for 16 of phenols **1**−**26**. Phenols **15** and **23** were considered outliers and were excluded from the solid correlation line: $E_{a,1} = 0.918$(O−H BDE) − 70.27 ($r^2 = 0.95$, eq X). The red square is for 2,4,6-tri*tert*butylphenol, **27**.

expect that the same would not hold true for the reaction of **dpph**• with phenols.

Kinetics and Mechanism of Reaction of 1,4-Cyclohexadiene, 28, with the dpph• Radical. It is commonly assumed that H-atom transfers from carbon to an oxidizing radical will occur purely by the HAT mechanism because the carbon atom from which the H-atom is derived has no lone pairs of electrons. This assumption has recently been challenged by one of us.[12b] A DFT study of the toluene/benzyl radical self-exchange reaction showed that $\pi-\pi$ stacking interactions permitted the PCET mechanism to operate, in addition to HAT, in this C−H---•C → C•---H−C self-exchange.[12b] A PCET mechanism also appears to be operating, to some extent, in the reaction of 1,4-cyclohexadiene with the **dpph**• radical. The transition-state structure for this reaction has the C−H bond pointing roughly toward the lone pair on the N• of the **dpph**• radical, see Figure 4, and to a lesser extent toward the orbital containing the unpaired electron. Additional images and animations of the TS SOMO orbital show significant $\pi-\pi$ stacking interactions between the incipient cyclohexadienyl radical and a phenyl group on the **dpph**•. Thus, the strong implication is that it is a proton that is transferred to the **dpph**• which, in turn, implies that the accompanying electron is drawn from the π-electron system of the hydrocarbon, rather than from the C:H bond.

Again we attribute the small *A*-factors, mentioned above, for the reaction of **dpph**• with **28** and **29** to steric protection of the N• of **dpph**• which greatly reduces the probability of reaction during radical/molecule encounters. It is noteworthy that the two heavy atoms between which the H-atom (proton) is transferred are separated in the TS by a much greater distance during the reaction of **dpph**• with 1,4-cyclohexadiene, **28**, R(C−H−N•) = 2.71 Å (see Figure 4) than they are during its reaction with phenols, e.g., R(O−H−N•) = 2.47 Å for 4-methoxyphenol (see Figure 3b). We attribute these large differences in heavy atom/heavy atom separation in the two TSs to the following factors:

(i) Much larger steric repulsion in the cyclohexadiene reaction because of its "face-on" approach to the lone pair on N• compared with the phenol reactions with their less sterically demanding "edge-on" approach to the lone pair on N•.

(ii) Formation of a pre-TS HB complex between the phenol's OH group and the lone pair on N• (Figure 2) will "draw" the O and N• atoms closer to one another than they would be in the absence of an HB complex.

(iii) A smaller atomic radius for oxygen than for carbon.

Evans−Polanyi Relationships. For a series of closely related reactions, the correlation, VIII, between E_a and reaction enthalpy for *exothermic* free-radical reactions was first reported by Evans and Polanyi[48a] and was further developed by Semenov.[48b]

$$E_a = \alpha\Delta H^0 + \beta \ (0 < \alpha < 1) \qquad \text{(VIII)}$$

The value of α is generally considered to be an indication of the position of the transition state along the reaction coordinate.[49] For exoergic reactions, $\alpha < 0.5$, and the transition state is "reactant-like" or "early". For endoergic reactions, $0.5 < \alpha < 1$, and the transition state is "product-like" or "late". Reaction 1 is endothermic for the majority of the phenols studied in the present work. If the Evans−Polanyi relation were to be accepted for these endothermic reactions, eq VIII could be rewritten as

$$E_{a,1} = \alpha\text{BDE(ArO-H)} + \text{constant} \qquad \text{(IX)}$$

This is because ΔH^0_1 = BDE(ArO-H) − BDE(**dpph**-H) = BDE(ArO-H) −78.9 kcal/mol.

Among phenols **1**−**27** there are 16 for which reliable ArO-H BDEs are available. Many are from experimental BDE measurements, and the rest (i.e., **5**, **6**, and **26**) were obtained using one[5a,22b] of the numerous additivity rules that describe the effect of substituents on ArO-H BDEs;[5a,10,22,30,50,51] see Table 1. The ArO-H BDE can also be calculated from the kinetics of reaction 1. For example, 3-methoxyphenol, **8**, has $k_1 = 1.4\ M^{-1}\ s^{-1}$ and $k_{-1} = 1.6 \times 10^5\ M^{-1}\ s^{-1}$ at 298 K (Table 1). Since the ΔS_1 is negligible[5a] and the BDE(**dpph**-H) = 78.9 kcal/mol,[5a] the ArO-H BDE for **8** = 78.9 − 0.59ln(1.4/1.6 × 10^5) = 85.7 kcal/mol. This BDE is in excellent agreement with a value of 86.2 kcal/mol (1 M standard state) obtained from DFT calculations on **8**; see Table 1 and ref 52.

The available ArO-H BDEs range from 77 to ca. 86 kcal/mol and are plotted against the measured activation energies from Table 1 (range 2−10 kcal/mol) in Figure 6. Provided the points for ubiquinol-0 (**15**), 2,2,5,7,8-pentamethyl-6-hydroxychroman (**23**), and 2,4,6-tri*tert*-butylphenol (**27**) are excluded,

(48) (a) Evans, M. G.; Polanyi, M. *Trans. Faraday Soc.* **1936**, *32*, 1333–1360. (b) Semenov, N. *Some Problems of Chemical Kinetics and Reactivity*; Pergamon Press: New York, 1958; Vol. 1.

(49) Fersht, A. R. *Proc. Natl. Acad. Sci. U.S.A.* **2004**, *101*, 14338–14342.

(50) (a) Mulder, P.; Saastad, O. W.; Griller, D. *J. Am. Chem. Soc.* **1988**, *110*, 4090–4092. (b) Jonsson, M.; Lind, J.; Erikson, T. E.; Merenyi, G. *J. Chem. Soc., Perkin Trans. 2* **1993**, 1567–1568.

(51) Many of the original ArO−H bond enthalpies10, 14, 22 were determined in benzene and contain an additional contribution from the enthalpy of the intermolecular H-bond between the phenol and benzene. This quantity is only ~1 kcal/mol[22d] for phenol itself and other phenols with "free" OH groups. It is negligible for hindered and intramolecularly H-bonded phenols.[22e] Measured ArO-H BDEs in the liquid-phase *must* also contain the enthalpy of solvation of the H• atom, ΔH_{sol}(H•), which is ~2.0 kcal/mol[22d] (almost independent of solvent). However, only a limited number of liquid-phase ArO−H BDEs reported in the literature contains this term.[14,22e] In those cases where H• atom solvation was obviously contained in the published ArO-H BDE these values were corrected for ΔH_{sol}(H•).

(52) Foti, M. C.; Daquino, C.; DiLabio, G. A.; Ingold, K. U. *J. Org. Chem.* **2008**, *73*, 2408–2411. Foti, M. C.; Daquino, C.; DiLabio, G. A.; Ingold, K. U. *J. Org. Chem.* **2008**, *73*, 7440.

(53) The ArO-H BDEs for **15** and **23** are known with considerable accuracy (<±1 kcal/mol),[14,22a−c] which suggests that these phenols are outliers because of "unusual" activation enthalpies. Indeed, the $E_{a,1}$ values for **15** and **23** are in the range for diffusion in nonviscous solvents[54] and have such small magnitudes that significant errors may be associated with their determination over the relatively small temperature range employed. Moreover, the reactions with **dpph**• of these two phenols are probably slightly exothermic and it seems highly improbable that exo- and endothermic reactions would fit the same $E_{a,1}$ vs ArO-H BDE correlation (see text).

as can easily be justified, [53−55] the plot of ArO-H BDE versus $E_{a,1}$ gives a rather satisfactory linear relation for most of the remaining phenols (see Figure 6), the equation being

$$E_{a,1}(\text{kcal/mol}) = 0.918\text{BDE(ArO-H)/kcal/mol} - 70.27\ (r^2 = 0.947)\ \text{(X)}$$

However, we consider it probable that there is not a truly *linear* Evans−Polanyi relation for reaction 1, *nor* for any other family of reactions, endothermic or exothermic, though there may appear to be linearity if the range of E_a and ΔH^0 are small.[49,57] This is because the Evans-Polanyi constant, α, will tend to 1 for strongly endothermic reactions and will decline to 0 for exothermic reactions when E_a approaches $E_{diffusion}$. The TS of reaction 1 moves along the reaction coordinate according to the sign and value of ΔH_1.[58] Reaction 1 is endothermic for most phenols in Chart 1 and a "product-like" TS is therefore to be expected, in agreement with the Hammond postulate.[58] The small deuterium kinetic isotope effect, (see Table 2) is also consistent with a product-like TS.[59] Accordingly, the Evans−Polanyi constant, α, is found to be relatively large, being ∼0.9 (see eq X).

Despite our misgivings about the theoretical validity of the Evans−Polanyi relation, Figure 6 leaves no doubt that for phenols having ArO-H BDEs in the range 80−87 kcal/mol, their BDEs can be correlated with the measured $E_{a,1}$ values via eq X. We have therefore employed eq X to estimate all the unknown ArO-H BDEs in the **1**−**26** set of phenols; see Table 1. We evaluate from Figure 2 that the level of accuracy for these BDEs is probably better than ±1 kcal/mol.

Conclusion

Theoretical calculations have revealed that the reaction of phenols with **dpph•** occurs via a single pathway by a mechanism that has both HAT and PCET character. These same calculations reveal that the mechanism for the reaction of **dpph•** with 1,4-cyclohexadiene *also* has a substantial degree of PCET character. In this reaction, the mechanism can be partially described as a process in which the C−H hydrogen is transferred as a proton to **dpph•** with the accompanying electron coming from the π-electron system of the diene. Thus, the PCET mechanism of H-atom transfer is more widespread than has been generally recognized (see also ref 12b).

Many previously unknown ArO-H BDEs have been determined by detailed kinetic studies of their reactions with **dpph•** over a 65 °C range of temperatures in cyclohexane. The activation energies of these reactions correlate linearly with the heats of reaction, ΔH_1, and with the ArO-H BDEs, as predicted by the Evans-Polanyi relationship. However, the validity of this relationship over a large range of ΔH, or ArO-H BDEs, is questioned because the position and energy of the TS along the reaction coordinate will vary with changes in ΔH. Despite this, over a limited range of ΔH the Evans−Polanyi relationship can still be useful.

Experimental Section

Synthesis of 7 and 14. 2,4-Dimethoxybenzaldehyde (1 g, 6 mmol) and *m*-chloroperbenzoic acid (mCPBA) (1.56 g, 9 mmol) were dissolved in 20 mL of anhydrous dichloromethane, and the solution was refluxed for 16 h. The solvent was then removed and the residue dissolved in ethyl acetate. The organic layer was washed with aqueous $NaHCO_3$ and with saturated brine and finally dried over Na_2SO_4. Removal of the solvent afforded the crude formate esters (as shown in the reaction below) of **7** and **14** which were then hydrolyzed (under nitrogen) in methanol/10% aqueous KOH (1:2 v/v) at room temperature for 1 h. The solution was then acidified with HCl 1 N and extracted (3 × 20 mL) with ethyl acetate. The organic layer was washed with water and saturated brine and finally dried over Na_2SO_4. The solvent was removed to give 880 mg of a crude residue which was purified by column chromatography on silica gel with cyclohexane/ethyl acetate (90:10 v/v) as eluent to give: 671 mg (72%) of 2,4-dimethoxyphenol (**7**) as a yellow oil and 26.1 mg (3%) of 2,4-dimethoxy-5-hydroxyphenol (**14**) as a white powder. Formation of minor quantities of **14** and 2,6-dimethoxy-3-hydroxyphenol with the above procedure is due to peracid oxidation of the aromatic ring.[60] The ESI-MS spectrum of **7**, in the negative ion-mode, showed a peak at 153 *m/z* $[M - H]^-$. ^{1}H NMR of **7** ($CDCl_3$): δ = 3.77 (s, 3H), 3.87 (s, 3H), 5.26 (s, 1H), 6.40 (dd, J = 8.6, 2.7 Hz, 1H), 6.50 (d, J = 2.7 Hz, 1H), 6.84 (d, J = 8.6 Hz, 1H). ^{13}C NMR ($CDCl_3$): δ = 55.6 (OCH_3), 55.7 (OCH_3), 3 × CH at 99.3, 104.2, 113.9; 3 quaternary C's at 139.6, 146.9, 153.4. The EI-MS of **14** showed peaks at *m/z*, 170 $[M]^+$, 155 and 127. ^{1}H NMR of **14** ($CDCl_3$): δ = 3.85 (s, 6H), 5.32 (s, 2H), 6.55 (s, 1H), 6.61 (s, 1H).

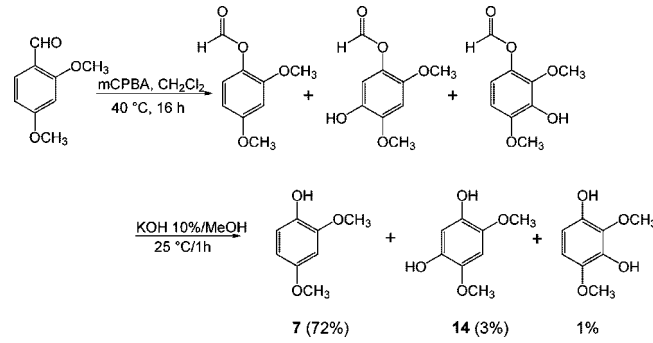

Synthesis of 12. Isovanillin (5 mmol, 760 mg) was added to a mixture of CH_2Cl_2 (10 mL), H_2O_2 (30%) (11 mmol, 1.3 mL), and SeO_2 (0.4 mmol 44 mg). The reaction mixture was allowed to react under stirring at room temperature for 16 h and then filtered. The filtrate was added to 20 mL of CH_2Cl_2, the organic layer was washed with 10 mL of 10% $NaHSO_3$, followed by 10 mL of 10% Na_2CO_3 and 10 mL of saturated brine, and was finally dried over Na_2SO_4. The solvent was removed and the residue hydrolyzed

(54) The activation energy for diffusion in cyclohexane is estimated to be approx. 2.6 kcal/mol This value was obtained from the self-diffusion coefficients for liquid cyclohexane reported in: Jonas, J.; Hasha, D.; Huang, S. G. *J. Phys. Chem.* **1980**, *84*, 109–112, using the equation $D/T = D_0 \exp(-E_D/RT)$.

(55) For 2,4,6-tri-*tert*-butylphenol, **27**, the ArO-H BDE is 80.1 kcal/mol[22a] and $E_{a,1}$ = 5.0 (± 0.5) kcal/mol (see Table 1), values that produce a point that falls well above the solid straight-line in Figure 2. This "deviation" is not due to some sterically-induced enhancement of $E_{a,1}$ because $E_{a,1}$ for **27** is equal, within experimental error, to $E_{a,1}$ for 2,4,6-trimethylphenol, **24** (see Table 1), and **24** lies essentially on the solid line in Figure 6. The "deviation" of **27** arises because steric repulsion between the OH group and the *o-tert*-butyl group to which it points weakens its ArO-H BDE bond (compared with the OH bond in **24**, for which the ring substituents' electronic effects must be similar, see Table 1) by about 1.5 kcal/mol.[56]

(56) (a) Ingold, K. U. *Can. J. Chem.* **1960**, *38*, 1092–1098. (b) Ingold, K. U.; Taylor, D. R. *Can. J. Chem.* **1961**, *39*, 471–480. (c) Ingold, K. U.; Taylor, D. R. *Can. J. Chem.* **1961**, *39*, 481–487. (d) Ingold, K. U. *Can. J. Chem.* **1962**, *40*, 111–121.

(57) Cohen, A. O.; Marcus, R. A. *J. Phys. Chem.* **1968**, *72*, 4249–4256. Marcus, R. A. *J. Phys. Chem.* **1968**, *72*, 891–899.

(58) Hammond, G. S. *J. Am. Chem. Soc.* **1955**, *77*, 334–338.

(59) DKIEs are largest for thermodynamically symmetrical TSs, (e.g., identity reactions, X• + XH → XH + X•) and are smaller for reactions having either an "early" or a "late" TS; see, e.g.: Pryor, W. A.; Kneipp, K. G. *J. Am. Chem. Soc.* **1971**, *93*, 5584–5586. Melander, L.; Saunders, W. H. *Reaction Rates of Isotopic Molecules*; Wiley: New York, 1980; Chapter 5.

(60) Bjørsvik, H.-R.; Occhipinti, G.; Gambarotti, C.; Cerasino, L.; Jensen, V. R. *J. Org. Chem.* **2005**, *70*, 7290–7296.

(under nitrogen) in a mixture of 10 mL of MeOH and 6 mL of 10% aqueous KOH at room temperature for 1 h. The solution was then acidified with HCl 1 N and extracted with ethyl acetate. The organic layer was washed with water and saturated brine and then dried over Na_2SO_4. After solvent removal, the residue (710 mg) was purified over silica gel using cyclohexane/ethyl acetate (80:20 v/v) as eluent to give 456 mg (60%) of 4-methoxyresorcinol (**12**) as a yellow oil. The EI-MS showed peaks at *m*/*z* 140 $[M]^+$, 125 and 97. ^{1}H NMR (MeOD): δ 3.81 (s, 3H), 5.5 (br, 2H), 6.31 (dd, J = 8.6, 2.6 Hz, 1H), 6.50 (d, J = 2.6 Hz, 1H), 6.69 (d, J = 8.6 Hz, 1H). ^{13}C NMR ($CDCl_3$): OCH_3 at δ 56.5; 3 × CH at 102.8, 105.8, 111.7; 3 quaternary C's at 140.8, 146.2 and 150.2.

Synthesis of 13. Reduction of 2,5-dimethoxy-1,4-benzoquinone with sodium dithionite ($Na_2S_2O_4$) in methanol/water at room temperature yielded phenol **13** in high yield. Briefly, approximately 150 mg of this benzoquinone was treated with a mix of ca. 10 mL of methanol and ca. 20 mL of water. The solution was degassed with nitrogen, and then an excess of $Na_2S_2O_4$ was added under stirring. After 15 min, another portion of $Na_2S_2O_4$ was added and the solution was left under bubbling nitrogen at room temperature until it gradually became colorless after approximately 1 h. The volume of the solution was reduced on a rotovap and then extracted with CH_2Cl_2 (3 × 10 mL). The organic phase was washed with water, dried on Na_2SO_4, and filtered and the solvent removed to afford ca. 130 mg of **13** (yield ca. 87%) as a white solid which slowly turned a pale pinkish. The solid was stored in the refrigerator at − 20 °C until use. ^{1}H NMR in DMSO-d_6: δ 3.64 (6H, s); 6.42 (2H, s) and 8.24 (2H, br s). ^{13}C NMR in DMSO-d_6: OCH_3 at δ 56.7; CH at δ 103.2; 2 quaternary Cs at δ 139.0 and 141.5. The UV−vis spectrum in EtOH shows a max at 259 nm.

Syntheses of 15−17. Ubiquinol-0, **15**, was obtained by reduction of ubiquinone-0 with ascorbic acid following the procedure reported in ref 61a.

The phenol (169 mg, 0.92 mmol) was then dissolved in anhydrous acetone (10 mL), and the solution was treated with Cs_2CO_3 (359 mg, 1.10 mmol), degassed with argon, and heated to ca. 60 °C. After a few minutes, ca. 200 μL of CH_3I was added under stirring, and the solution was left to reflux for about 3 h under argon. The color of the solution slowly changed from dark green (after the addition of Cs_2CO_3) to yellow at the end of the reaction. The solution was then acidified with 2 N HCl and extracted (3 × 10 mL) with CH_2Cl_2. The organic phase was in turn extracted (3 × 10 mL) with an aqueous solution of 2 N NaOH to separate the dimethylated from the monomethylated ethers of ubiquinol-0. The aqueous phase (containing the monomethylated ethers) was acidified with 2 N HCl and re-extracted (3 × 10 mL) with CH_2Cl_2 to give ca. 70 mg of a crude residue which was purified on a preparative TLC plate. This was initially eluted with cyclohexane/acetone 90:10 v/v (to remove the last traces of the dimethylated ether) and then with CH_2Cl_2/cyclohexane/acetone 70:27:3 v/v to yield 39.4 mg (23%) of **16** and 2.4 mg (1.4%) of **17** as yellow oils. The structure of the isomer **16** was confirmed by NOESY experiments which showed a correlation between the ring proton (6.44 ppm; see below) and one OCH_3 (3.80 ppm; see below) and the absence of any correlation between the ring methyl (2.21 ppm; see below) and one OCH_3. ^{1}H NMR of **15** ($CDCl_3$): δ 2.18 (3H, d, J = 0.6 Hz); 3.89 (3H, s) and 3.92 (3H, s); ca. 5.3 (2H, br); 6.49 (1H, br q). ^{1}H NMR of **16** (CDCl3): δ 2.21 (3H, s); 3.80 (3H, s); 3.87 (3H, s) and 3.95 (3H, s); 6.44 (1H, s); ca. 5.4 (1H, br). ^{13}C NMR of **16** ($CDCl_3$): CH_3 at δ 15.3; 3 × OCH_3 at 56.5, 60.72 and 61.0; CH at 109.5; 4 quaternary C's at 117.8, 139.8, 141.0, 145.8. ^{1}H NMR of **17** ($CDCl_3$): δ 2.19 (3H, s); 3.78 (3H, s); 3.92 (3H, s); 3.93 (3H, s); 6.50 (1H, s). ^{13}C NMR of **17** ($CDCl_3$): CH_3 at δ 15.4; 3 × OCH_3 at 60.4, 60.5 and 61.0; CH at 110.5; quaternary C's at 126.7, 131.1, 137.9, 144.7. The EI-MS spectra of **16** and **17** showed the following main peaks at *m*/*z* 198 $[M]^+$, 183, and 140.

Synthesis of 18. This phenol was prepared (46% yield) according to the procedure reported in ref 61b and summarized in the following reaction scheme.

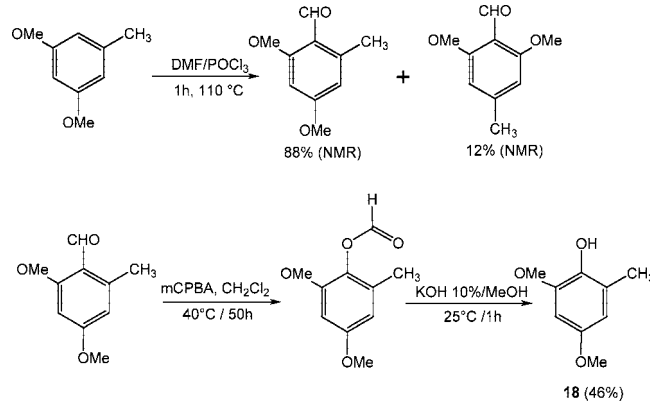

The final crude residue of reaction containing **18** was purified by column chromatography on silica gel using cyclohexane/ethyl acetate (90:10 v/v) as eluent to give 2,4-dimethoxy-6-methylphenol, **18**, as a white powder in 46% final yield. The EI-MS showed peaks at *m*/*z* 168 $[M]^+$, 153, 125. ^{1}H NMR ($CDCl_3$): δ = 2.26 (s, 3H), 3.76 (s, 3H), 3.86 (s, 3H), 5.30 (s, 1H, OH), 6.30 (d, J = 2.7 Hz, 1H), 6.36 (d, J = 2.7 Hz, 1H).^{13}C NMR ($CDCl_3$): δ = 15.4 (CH_3), 55.5 (OCH_3), 55.8 (OCH_3), 96.7 (CH), 106.6 (CH) and 4 quaternary C's at 123.6, 137.7, 146.5, 152.5.

Kinetics. Solutions of **dpph•** were prepared in cyclohexane or *n*-hexane at a concentration of ca. (2 − 10) × 10^{-5} M by sonicating (at room temperature) the mixture until all **dpph•** crystals were dissolved. Phenols were dissolved in cyclohexane or *n*-hexane at a final concentration of 1−5 mM. To facilitate the dissolution of the most polar phenols, small quantities of CH_2Cl_2 or ethyl acetate (<2% vol) were added. The reservoir syringes of the stopped-flow spectrophotometer were filled with the solutions which were then purged at room temperature with dry nitrogen for 5 min at a low flow rate (the concentrations were corrected for solvent evaporation). During the purge phase, the solutions were transferred back and forth into the drive syringes to remove the oxygen adsorbed into the syringes. Then, the drive-syringes were filled and the solutions were allowed to stand for 15 min for thermal equilibration. Each single rate constant at a given temperature was obtained by averaging the values obtained from three to six decay traces at 512nm. The observed deviations from the average were smaller than ± 10%. The explored temperature range was 5 to 70 °C and phenol concentrations were corrected for solvent expansion using an averaged cubic expansion coefficient of 1.2 × 10^{-3} °C^{-1} for cyclohexane and of 1.45 × 10^{-3} °C^{-1} for *n*-hexane. The program SPECFIT (version 3.0.34) was used to make the simulations (see text) of a few experimental traces.

The kinetics of reaction of the hydrocarbons **28** and **29** (TH_2) with **dpph•** were complicated by autocatalytic phenomena. Indeed, the rate of reaction, -d[**dpph•**]/d*t*, with $[TH_2] \gg$ [dpph•] accelerated as the dpph• radical was consumed.[62] This autocatalysis cannot be attributed to a double bond shift to form a more reactive 1,3-cyclohexadienes since the rate constant for reaction of **dpph•** with 1,3-cyclohexadiene was found to be smaller than that for reaction with 1,4-cyclohexadiene. We consider it most likely that the initial TH• radical may self-quench with formation of a more reactive TH−TH dimer and $(TH)_n$ oligomers (reaction of 1,3-cyclohexadiene with **dpph•** gave a white polymer). Rate constants for the reaction of **28** and **29** with **dpph•** were therefore determined from initial rates.

Acknowledgment. G.A.D. thanks the Program for Energy Research (PERD) for funding, the Centre for Excellence in Integrated Nanotools, the Academic Information and Communication Technologies (AICT), and Professor Pierre Boulanger (all of the University of Alberta) for access to computing resources. M.C.F. thanks Dr. Paolo Bovicelli (CNR, Rome) for

kindly providing samples of phenol **5**. We are grateful to Annick Le Quellec, Christian DiLabio, and Justin DiLabio for contributing to the animations provided in the Supporting Information. Dr. Jon Johansson's help in preparing the animations is also appreciated.

Supporting Information Available: Optimized Cartesian coordinates for **dpph•**, the hydrogen bonded structure involving the N• center of **dpph•** and 4-methoxyphenol, and the structures of hydrogen transfer transition states involving phenol, 3-methoxyphenol and 4-methoxyphenol with **dpph•**, with the corresponding locally dense basis set assignments, details of some hydrogen bonded complexes of 4-methoxyphenol with **dpph•**, and additional experimental details. Animations showing more detailed views of the orbitals illustrated in Figures 3 and 4 are also provided. This material is available free of charge via the Internet at http://pubs.acs.org.

JO8016555

(61) (a) Foti, M.; Ingold, K. U; Lusztyk, J. *J. Am. Chem. Soc.* **1994**, *116*, 9440–9447. (b) Godfrey, I. M.; Sargent, M. V.; Elix, J. A. *J. Chem. Soc., Perkin Trans. 1* **1974**, 1353–1354.

(62) The decay traces at 512 nm were oriented with the convexity toward the abs axis.